

Communications



CO₂ Reduction

How to cite: *Angew. Chem. Int. Ed.* **2023,** *62*, e202215213
International Edition: doi.org/10.1002/anie.202215213
German Edition: doi.org/10.1002/ange.202215213

Aqueous Photoelectrochemical CO₂ Reduction to CO and Methanol over a Silicon Photocathode Functionalized with a Cobalt Phthalocyanine Molecular Catalyst

Bo Shang, Conor L. Rooney,* David J. Gallagher, Bernie T. Wang, Andrey Krayev, Hadar Shema, Oliver Leitner, Nia J. Harmon, Langqiu Xiao, Colton Sheehan, Samuel R. Bottum, Elad Gross, James F. Cahoon, Thomas E. Mallouk, and Hailiang Wang*

Abstract: We report a precious-metal-free molecular catalyst-based photocathode that is active for aqueous CO₂ reduction to CO and methanol. The photoelectrode is composed of cobalt phthalocyanine molecules anchored on graphene oxide which is integrated via a (3aminopropyl)triethoxysilane linker to p-type silicon protected by a thin film of titanium dioxide. The photocathode reduces CO₂ to CO with high selectivity at potentials as mild as 0 V versus the reversible hydrogen electrode (vs RHE). Methanol production is observed at an onset potential of -0.36 V vs RHE, and reaches a peak turnover frequency of 0.18 s⁻¹. To date, this is the only molecular catalyst-based photoelectrode that is active for the six-electron reduction of CO₂ to methanol. This work puts forth a strategy for interfacing molecular catalysts to p-type semiconductors and demonstrates state-of-the-art performance for photoelectrochemical CO₂ reduction to CO and methanol.

[*] B. Shang, C. L. Rooney, D. J. Gallagher, B. T. Wang, O. Leitner, N. J. Harmon, H. Wang Department of Chemistry, Yale University New Haven, CT 06520 (USA) and Energy Sciences Institute, Yale University West Haven, CT 06516 (USA) E-mail: conor.rooney@yale.edu

A. Krayev

HORIBA Instruments Inc.

hailiang.wang@yale.edu

359 Bel Marin Keys Blvd, Suite 18, Novato, CA 94949 (USA)

H. Shema, E. Gross

Institute of Chemistry and Center for Nanoscience and Nanotechnology, Hebrew University of Jerusalem

Jerusalem, 91904 (Israel)

L. Xiao, C. Sheehan, T. E. Mallouk Department of Chemistry, University of Pennsylvania Philadelphia, PA 19104 (USA)

S. R. Bottum, J. F. Cahoon

Department of Chemistry, University of North Carolina at Chapel Hill

Chapel Hill, NC 27599-3290 (USA)

Anthropogenic CO₂ emissions and their contribution to climate change have made the development and implementation of carbon-neutral energy generation and storage a global priority. The United Nations Paris Agreement targets a 45% reduction in global emissions by 2030 and carbonneutrality by 2050.[1] As a potential carbon-neutral or carbon-negative technology, electrochemical CO2 reduction reactions convert the greenhouse gas into value-added chemical building blocks or liquid fuels by using only water and electricity as additional inputs. [2] Photoelectrocatalytic (PEC) CO₂ reduction further lowers the energy input by harvesting solar energy in tandem with an applied voltage.^[3] Major challenges of the CO₂ reduction reaction are its slow kinetics, low selectivity owing to the plurality of possible products, and competition for electrons by the hydrogen evolution reaction (HER). As the key to lowering the overpotential and achieving high activity and selectivity towards a single CO2 reduction product, a variety of catalysts have been explored for modification of the photocathode in the PEC CO₂ reduction reaction.^[4,5] Among them, molecular catalysts are advantageous due to their well-defined structures, which are readily modified to tailor the reaction kinetics. Their detailed reaction mechanisms can also be probed by the well-developed tools of molecular chemistry. A number of molecular catalysts have been deposited on semiconductor surfaces for PEC CO2 reduction and have shown promising activity. [6-10] However, many of these systems require noble metal catalysts or expensive compound semiconductors, which makes the cost of the PEC electrode high.

Si is a preferred photo-absorber for PEC CO₂ reduction because of its low cost and well-studied properties as the backbone of the semiconductor industry. Many molecular catalysts have been studied in the solution phase with Si photocathodes, [11-14] but in this configuration, the catalyst must diffuse to and from the photoelectrode and the achievable catalytic rates are therefore low. The development of a high-performance and low-cost Si photocathode with an anchored molecular catalyst for selective PEC CO₂ reduction in aqueous media remains a largely unmet challenge. A few recent reports have made progress towards this goal. Reisner et al. developed a photocathode consisting of p-type Si (p-Si) coated with a mesoporous TiO₂ layer and





functionalized with cobalt bis(terpyridine) anchored via phosphonate groups. The resulting photoelectrode is active for PEC CO2 reduction in a mixture of acetonitrile and water, producing a photocurrent of about $-0.18\,\mathrm{mA\,cm^{-2}}$ with Faradaic efficiencies (FEs) for CO and formate of 48 % and 13 % respectively. [15] In a subsequent study, the Reisner group used the same anchoring strategy for phosphonated cobalt phthalocyanine (CoPcP) and demonstrated improved performance in fully aqueous PEC CO₂ reduction. The p-Si mesoTiO₂|CoPcP photoelectrode achieves a photocurrent of $-0.15 \,\mathrm{mA\,cm^{-2}}$ and a FE_{CO} of 66 % with the assistance of a bias of $-0.11\,\mathrm{V}$ vs the reversible hydrogen electrode (RHE), representing the state-of-the-art p-Si photocathode functionalized with a molecular catalyst for CO₂ reduction.^[7] Higher performance was realized by Li and co-workers with p-n junction Si. [6] These findings open the door for further investigation to improve the rate and selectivity of PEC CO₂ reduction not only to CO but also to more deeply reduced products.

Recent work from our group has demonstrated that the immobilization of cobalt phthalocyanine (CoPc) molecules onto carbon nanotubes (CNTs) enhances their electrocatalytic performance. The planar aromatic ligand structure of CoPc enables non-covalent π - π stacking with the graphitic carbon surface. This strong electronic interaction promotes highly dispersed CoPc molecules on the CNT surface and fast electron transfer from the electrode to the active site. The CoPc/CNT catalyst produces CO with > 95 % FE at low overpotential in electrochemical CO₂ reduction.^[16] Remarkably, at more negative applied potentials this hybrid catalyst is active for the six-electron reduction of CO2 to methanol (MeOH) with FE higher than 40 %.[17] CoPc/CNT is one of the very few molecular catalysts demonstrated to reduce CO₂ by greater than two electrons with appreciable activity and selectivity. Nevertheless, the six-electron reduction of CO2 to MeOH over a molecular catalyst on Si-based photocathodes has not been reported to date.

In this work, we develop a p-Si photocathode interfaced with CoPc molecules immobilized on graphene oxide (GO/ CoPc) for PEC CO2 reduction to CO and MeOH. Our photocathode architecture is composed of p-Si protected by a 2 nm thick film of TiO₂, functionalized with (3aminopropyl)triethoxysilane (APTES), and coated with the GO/CoPc catalyst. Each component of this architecture makes an indispensable contribution to the PEC performance. The assembled photoelectrode shows CO production in a near neutral aqueous electrolyte at 0 V vs RHE (all potentials in this work are referenced to RHE unless otherwise stated) and reaches a maximum FE_{CO} of 86 % and a current density of 0.5 mA cm^{-2} at -0.19 V under 1.5 sunillumination (300 W Xe lamp, 400 nm cut-off). MeOH is generated at an onset potential of $-0.36\,\mathrm{V}$ and reaches a maximum FE of 8% at -0.62 V. This work sets a new benchmark performance for p-Si photocathodes modified with a molecular catalyst in aqueous PEC CO₂ reduction to CO, as well as the photoelectrochemical production of MeOH for the first time at illuminated p-Si electrodes.

The GO/CoPc catalyst was assembled by non-covalent π - π stacking similar to our previously developed method for

immobilization of CoPc on CNTs. First, GO was prepared by a modified Hummer's method (Supporting Information section 1.a). CoPc molecules were then assembled onto the GO flakes by ultrasonication in N,N-dimethylformamide (DMF) (Figure 1a). GO serves as a conductive support to enable molecular-level dispersion of CoPc and facilitate electron conduction. [18] Inductively coupled plasma mass spectrometry (ICP-MS) was used to determine the CoPc loading on the GO. The Co loading was found to be 0.24 wt.%, corresponding to a CoPc loading of 2.3 wt.%. Atomic force microscopy (AFM) identifies GO/CoPc flakes with an average lateral size of $\approx 1 \,\mu m$ (Figure 1b-d). Tipenhanced Raman spectroscopy (TERS) was employed to further characterize the distribution of the CoPc molecules on GO (Figure 1e-f). TERS mapping, using the strongest Raman feature of CoPc at 1530 cm⁻¹ (Figure S1), confirmed the relatively uniform distribution of CoPc molecules on GO (Figure 1e).^[19] The corresponding Raman spectrum of the hybrid catalyst shows clear combined features of CoPc and GO (Figure 1f). [20] These results confirm the successful assembly of CoPc on GO.

The preparation of Si-based GO/CoPc photoelectrodes was achieved in a stepwise assembly. First, a lightly doped ptype Si wafer (B doped, $1-10 \Omega cm$), pre-cleaned with a buffered HF solution to remove the surface oxide layer, was coated with 2 nm TiO₂ as a surface protection layer by atomic layer deposition (ALD) (Supporting Information section 1.c). The Si-TiO₂ wafers were cut into squares with 1 cm² area and treated with an APTES solution, during which the APTES molecules react with TiO2 surface oxygen groups via silanization, leaving the free amine groups of the molecules exposed. [21] Finally, the Si-TiO₂-APTES (STA) substrate was soaked in a GO/CoPc aqueous dispersion to form a monolayer-like coating on the surface with the aid of electrostatic and hydrogen bonding interactions between the APTES amine groups and the GO carboxylic acid groups (Figure 2a). [22] After each coating step, the contact angle of water on the substrate decreases, indicating successful functionalization of APTES and GO/CoPc on the substrate (Figure S2). Scanning electron microscopy (SEM) and AFM images in Figure 2b-c confirm the uniform distribution on the micrometer scale of GO/CoPc flakes on STA. To provide more catalytic sites for CO₂ reduction, 0.05 mg of GO/CoPc was further drop-cast onto the 1 cm² photoelectrode, resulting in an approximately 600 nm thick catalyst layer (Figure 2d-e). The prepared photoelectrode is denoted as STA-GO/CoPc.

The electrocatalytic activity of GO/CoPc deposited on carbon fiber paper (CFP-GO/CoPc) and the PEC activity of STA-GO/CoPc for CO₂ reduction were evaluated in 0.1 M KHCO₃ aqueous electrolyte. Prior to all catalytic tests, electrodes were subjected to a mild reductive potential under inert atmosphere, which was done to partially reduce the GO layer (Figure S3). Electrocatalytic tests were performed in a custom-made H-cell with gas products analyzed by in-line gas chromatography and liquid products detected by ¹H NMR after the 30-min reaction (Figures 3a, S4, S5). In dark electrochemistry, CFP was chosen to be the substrate because it is electrically conducting as opposed to

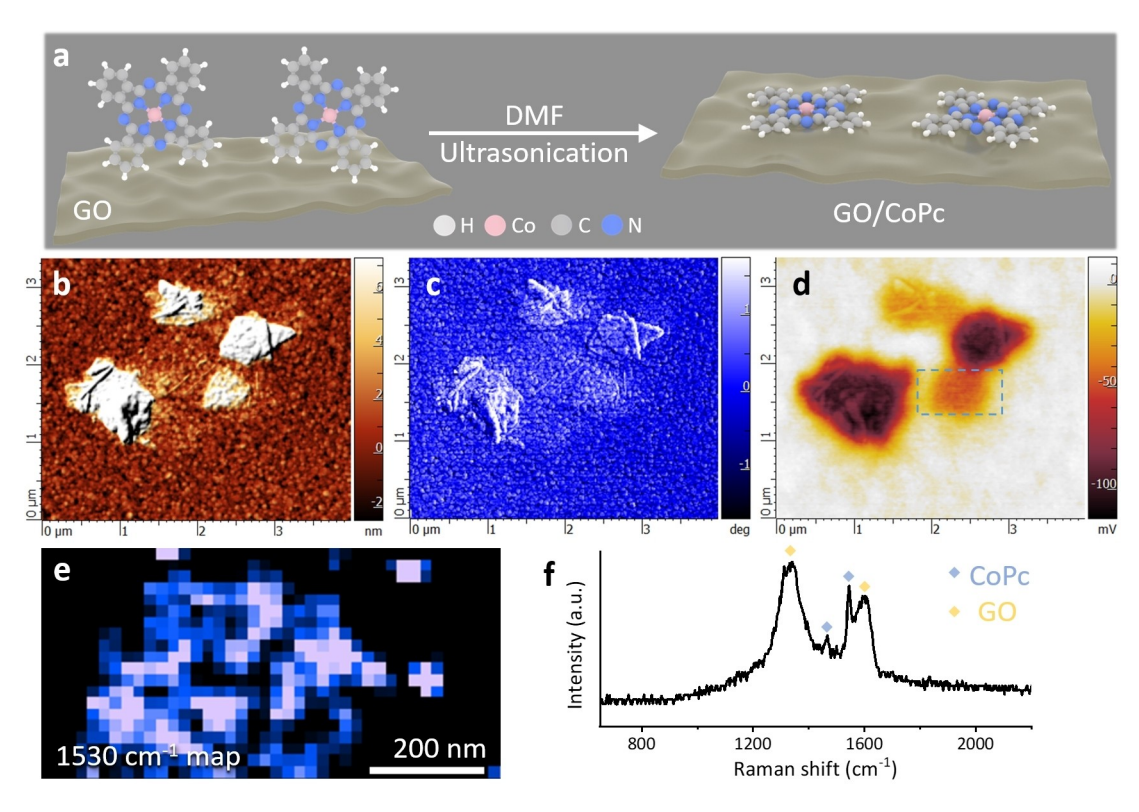


Figure 1. (a) Schematic depiction of the assembly method of CoPc molecules on GO. (b–d) AFM topology, phase, and contact potential difference images. (e) TERS mapping of 1530 cm⁻¹ Raman shift of the blue dashed square in (d). (f) TERS spectra averaged over the area of (e), the blue and yellow peaks show the Raman features of CoPc and GO, respectively.

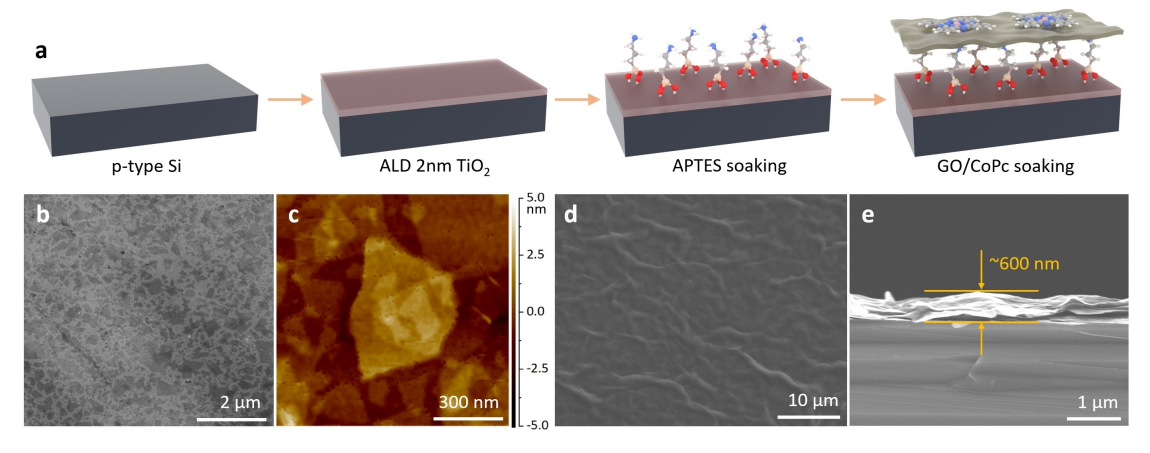


Figure 2. (a) Illustration of STA-GO/CoPc assembly procedure. Atom representative colors: red, O; yellow, Si; gray, C; white, H; blue, N; pink, Co. (b–c) SEM and AFM images of STA-monolayer GO/CoPc. (d) Top-view and (e) cross-section SEM images of STA-GO/CoPc.

the semiconducting p-Si. The CFP-GO/CoPc electrode produces CO at an onset of -0.5 V and reaches a peak FE $_{\rm CO}$ of 82% at -0.7 V (Figure 3b). The electrochemical CO $_{\rm 2}$ reduction performance of the GO/CoPc catalyst is similar to that in our previous work on CoPc immobilized on CNTs, despite a lower current which may be attributed to the lower conductivity of GO compared to CNTs. [16] To investigate the PEC performance of GO/CoPc, the STA-GO/CoPc assembly was first back-contacted with a metal wire using In-Ga eutectic and silver paste. Then the backside (including the

metal contact) of the PEC electrode was sealed with vacuum wax to allow only the front surface of the assembly to be exposed to the electrolyte (Figure S6). The same setup of the electrochemical cell was used for PEC CO₂ reduction except for a quartz window in the cathode compartment to allow illumination onto the photoelectrode (Figure 3c). A 300 W Xe lamp was used as the light source and a UV filter was applied to remove wavelengths shorter than 400 nm in all experiments. Light intensity was calibrated to 1.5 suns for all PEC measurements unless otherwise specified. Interest-

5213773, 2023, 4, Downloaded from https://onlinelibrary.wiley.com/doi/10.1002/anie.20215213 by Yale University, Wiley Online Library on [08/06/2023]. See the Terms and Conditions (https://onlinelibrary.wiley.com/terms-and-conditions) on Wiley Online Library for rules of use; OA articles are governed by the applicable Creative Commons Licensed

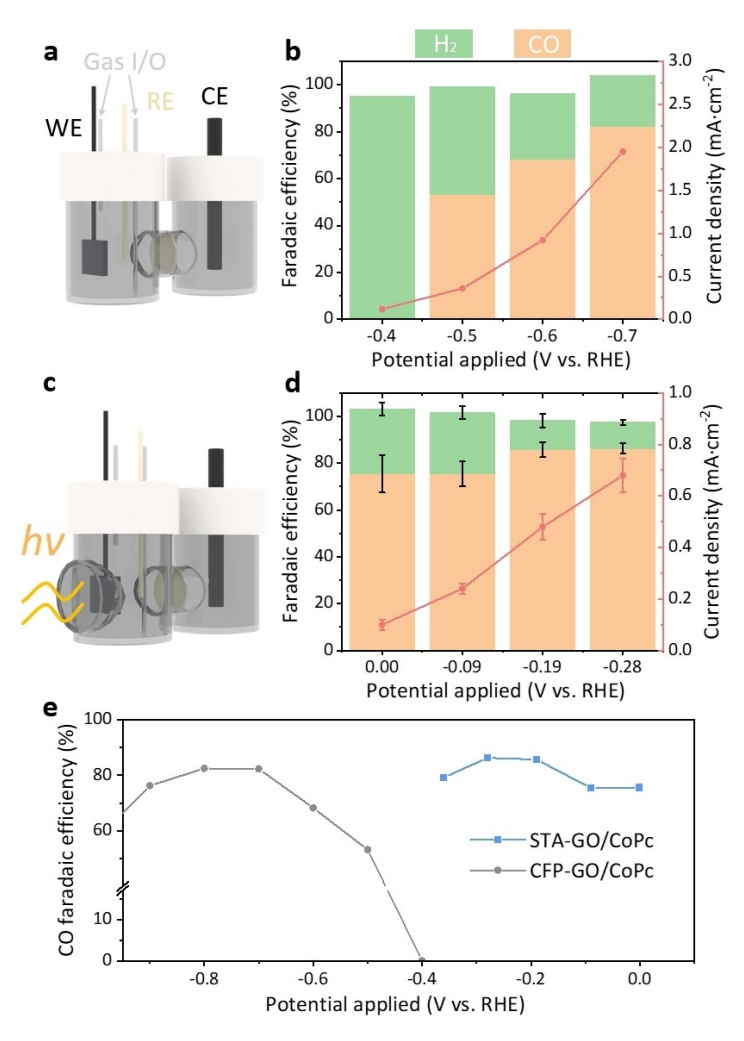


Figure 3. (a) Illustration of the electrochemistry H-cell. The label shows the working electrode (WE), counter electrode (CE), reference electrode (RE), and gas in/out ports. (b) FE of CO, H₂, and current density of CFP-GO/CoPc with different applied potentials. (c) Illustration of the PEC H-cell with a quartz window and side illumination. (d) FE of CO, H₂, and current density of STA-GO/CoPc with different applied potentials under 1.5 sun illumination. (e) Comparison of CO selectivity between STA-GO/CoPc (PEC CO₂ reduction) and CFP-GO/CoPc (electrochemical CO₂ reduction).

ingly, even at a 0 V applied bias, the STA-GO/CoPc shows a high FE $_{\rm CO}$ of 76%. At an applied potential of -0.28 V, the STA-GO/CoPc achieves a maximum FE $_{\rm CO}$ of 86% with a photocurrent density of $0.7~{\rm mA\,cm^{-2}}$ (Figure 3d), which compares favorably to previous reports based on molecular catalysts on p-Si, and is comparable to studies using large-band gap semiconductors under such low overpotentials (Table S1). [6-15,23,24]

To attain the same FE_{CO}, the overpotential on STA-GO/CoPc was more than 0.5 V lower compared to CFP-GO/CoPc (Figure 3e), which can be attributed to the photovoltage contribution from p-Si. Although STA-GO/CoPc gives a lower current density than CFP-GO/CoPc, it is worth noting that the catalyst loading on the STA-GO/CoPc samples was eight times lower, which is necessary to prevent the catalyst layer from peeling off during the PEC tests (Figure S7). Assuming that every CoPc molecule on the photocathode is active, the CO turnover frequency (TOF) of STA-GO/CoPc is calculated to be 1.5 s⁻¹ at -0.28 V,

which is higher than the $0.5\,\mathrm{s}^{-1}$ determined for CFP-GO/CoPc at $-0.7\,\mathrm{V}$ (Supporting Information section 2.f). The higher TOF on the photoelectrode can be attributed to the lower loading of CoPc. [25] These results demonstrate that the STA-GO/CoPc photoelectrode architecture provides highly efficient catalytic active sites for PEC CO₂ reduction.

At higher overpotentials, GO/CoPc, like CoPc/CNT in our previous work, [17] is active for the six-electron reduction of CO₂ to MeOH. In dark electrochemistry, CFP-GO/CoPc yields MeOH at an onset potential of -0.8 V and reaches an optimal FE_{MeOH} of 23 % at -1.0 V (Figure 4a). In the PEC case, we find that the STA-GO/CoPc photoelectrode generates MeOH at a much lower onset potential of -0.36 V and reaches a peak FE_{MeOH} of 8% at -0.62 V (Figure 4b). The 13 C isotopic labeling experiment confirms that CO₂ is the MeOH source (Figure S8). At -0.62 V, STA-GO/CoPc produces MeOH with a TOF of 0.18 s⁻¹, which is similar to the TOF for MeOH of CFP-GO/CoPc at -1.0 V measured to be 0.21 s⁻¹. We propose that the

5213773, 2023, 4, Downloaded from https://onlinelibrary.wiley.com/doi/10.1002/anie.20215213 by Yale University, Wiley Online Library on [08/06/2023]. See the Terms and Conditions (https://onlinelibrary.wiley.com/terms-and-conditions) on Wiley Online Library for rules of use; OA articles are governed by the applicable Creative Commons Licensed

а

Faradaic efficiency (%)

100

80

60

40

20

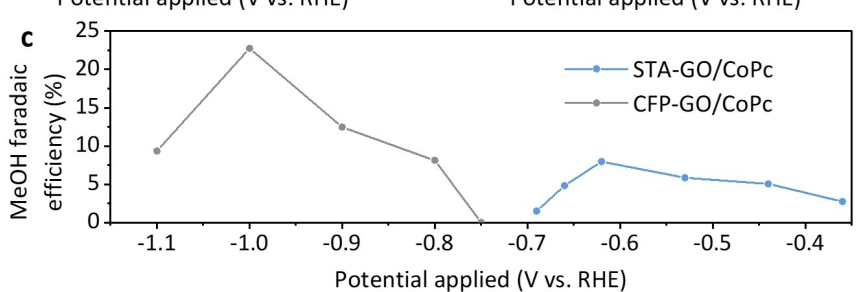


Figure 4. (a) FE of CO, H₂, methanol, and current density of CFP-GO/CoPc with different applied potentials under 1.5 sun illumination. (b) FE of CO, H₂, methanol, and current density of STA-GO/CoPc with different applied potentials under 1.5 sun illumination. (c) Comparison of MeOH selectivity (FE) between STA-GO/CoPc (PEC CO₂ reduction) and CFP-GO/CoPc (electrochemical CO₂ reduction) under varied applied potential.

mechanism of MeOH formation in the PEC reaction is likely to be the same as in electrocatalytic CO₂ reduction, and that CO is the key intermediate to the formation of MeOH. $^{[17,26\text{--}28]}$ The optimal potential for FE $_{\text{MeOH}}$ of STA-GO/CoPc is about 0.4 V lower than that of CFP-GO/CoPc (Figure 4c), demonstrating the photovoltage contribution from the Si to the catalyst. The lower optimal FE_{MeOH} on STA-GO/CoPc compared with CFP-GO/CoPc may be due in part to the planar structure of the Si substrate; that is, the planar electrode is not able to trap the electrogenerated CO intermediate near its surface for further reduction as effectively as the porous CFP electrode. The lower catalyst loading, which leads to a slower rate of CO generation, may be another contributor. We hypothesize that improved MeOH selectivity may be accomplished by Si surface morphology engineering, which can be done using established techniques such as chemical treatment photolithography, [29] to increase surface roughness and manufacture porous Si for higher catalyst loadings and improved CO retention. Alternatively, gas diffusion layers can be employed as a top layer on the photoelectrode surface to increase mass transport of gas reactants to the active site. We will explore these strategies in future work. In summary, for dark electrocatalytic CO2 reduction, CFP-GO/CoPc shows peak CO selectivity of 82 % at −0.7 V and peak MeOH selectivity of 23 % at -1.0 V. For PEC CO₂ reduction, STA-GO/CoPc shows peak CO selectivity of 86% at $-0.28\,\mathrm{V}$ and peak MeOH selectivity of 8% at -0.62 V. This is the first example of successful integration of a molecular catalyst on Si for PEC CO2 reduction to MeOH, and demonstrates the potential of molecular catalysis for greater than two-electron reduction of CO2 on Si photocathodes.

The stability of the STA-GO/CoPc photocathode for PEC production of CO and MeOH from CO2 was tested under 1 sun illumination to better simulate real-world conditions. At an applied potential of -0.19 V, the photoelectrode shows a stable FE_{CO} of around 86% and only slight decay in current density over 6 hours of continuous operation (Figure 5a). The FE_{CO} and photocurrent are comparable to the result from 30 min controlled potential photoelectrolysis under 1.5 suns (Figure 3d). At an applied potential of -0.62 V, the photocathode generates MeOH with a FE of 6% for the first hour (Figure 5b), which is slightly lower than that from the 30 min measurement under 1.5 suns (Figure 4b). FE_{MeOH} continues to decrease over the next two hours along with a concurrent increase in HER. This decay is likely due to the partial detachment of the catalyst layer caused by bubble generation and/or degradation of the APTES layer, [30] which might expose HER-active sites on the Si surface. The stability tests under 1.5 sun illumination show similar results but with a slightly quicker decay in catalytic activity (Figure S9). We hypothesize that this detachment problem can be solved by engineering the Si surface to increase the surface roughness and improve the adhesion between catalyst film and substrate.

Admittedly, interfacing the hydrophilic GO/CoPc film on the smooth hydrophobic Si surface was a significant obstacle in this work (Table S2). If the TiO₂ layer is omitted (Si with the native oxide layer as the substrate), the current 5213773, 2023, 4, Downloaded from https://onlinelibrary.wiley.com/doi/10.1002/anie.20215213 by Yale University, Wiley Online Library on [08/06/2023]. See the Terms and Conditions (https://onlinelibrary.wiley.com/terms-and-conditions) on Wiley Online Library for rules of use; OA articles are governed by the applicable Creative Commons License

Figure 5. Stability tests of STA-GO/CoPc under (a) -0.19 V and (b) -0.62 V with 1 sun illumination.

Time (h)

drops to one-tenth of the current under optimal conditions, suggesting that charge recombination at the native oxide layer may be the dominant kinetic pathway (Figure S10). If the APTES binding layer is omitted, the GO/CoPc quickly peels off the electrode and a low current and FE_{CO} is obtained (Figures S11, S12). Without the drop-cast thick catalyst layer, the current and FE_{CO} are also low because of the limited number of catalytically active sites and the uncovered STA surface, which is active for HER (Figures S13, S14). Notably, replacing GO/CoPc with the CNT/ CoPc catalyst resulted in a significant decrease in the photocurrent and stability, which can be explained by the high optical density of CNT (thus less light can reach the Si surface to generate electron-hole pairs) and the absence of interaction between CNT and APTES (Figure S15). Together, each layer of the STA-GO/CoPc plays a critical role in achieving high-performance PEC CO2 reduction. The quantum efficiency (QE) of STA-GO/CoPc was tested using a power-adjustable 730 nm LED (Supporting Information section 2.c). The maximum QE values under low illumination power at applied potentials of -0.2 V and -0.7 V were 6.5% and 40.6%, respectively (Figure S16). When the illumination power was increased, the QE was observed to drop rapidly. This may indicate that charge separation of p-Si or the catalyst turnover rate may be limiting the QE under high-power illumination, limitations that could be overcome by constructing p-n junction photocathodes or by developing more active catalyst materials. [6,17,31]

In summary, for the first time, we demonstrate aqueous PEC $\rm CO_2$ reduction to MeOH at a molecular catalyst-modified Si photocathode. Additionally, the as-constructed STA-GO/CoPc photoelectrodes produce CO with high selectivity at ultralow overpotential owing to a photovoltage estimated to be greater than 0.5 V. The onset potential of CO generation is 0 V and an optimal FE $_{\rm CO}$ of 86% is achieved. Under higher applied potentials of -0.36 V to -0.62 V, MeOH emerges as a liquid product with FE $_{\rm MeOH}$ up to 8%. This study thus serves as a starting point for multi-electron PEC $\rm CO_2$ reduction to liquid fuels at low overpotentials on hybrid photoelectrodes based on molecular catalysts on Si.

Acknowledgements

This work was supported as part of the Center for Hybrid Approaches in Solar Energy to Liquid Fuels (CHASE), an Energy Innovation Hub funded by the U.S. Department of Energy, Office of Science, Office of Basic Energy Sciences under Award Number DE-SC0021173. The AFM characterization work was supported by U.S. National Science Foundation grant no. 2129963 and U.S.-Israel Binational Science Foundation grant no. 2021671. We thank Dr. Li Wang and Prof. Menachem Elimelech for their help with the contact angle measurments.

Conflict of Interest

The authors declare no conflict of interest.

Time (h)

Data Availability Statement

The data that support the findings of this study are available from the corresponding author upon reasonable request.

Keywords: CO_2 Reduction · Methanol · Molecular Catalyst · Photoelectrochemical Reaction · Silicon Photocathode

- [1] S. M. Jordaan, C. Wang, Nat. Catal. 2021, 4, 915–920.
- [2] M. B. Ross, P. De Luna, Y. Li, C.-T. Dinh, D. Kim, P. Yang, E. H. Sargent, *Nat. Catal.* 2019, 2, 648–658.
- [3] D. Li, K. Yang, J. Lian, J. Yan, S. Liu, Adv. Energy Mater. 2022, 12, 2201070.
- [4] X. Chang, T. Wang, P. Yang, G. Zhang, J. Gong, Adv. Mater. 2019, 31, 1804710.
- [5] N. Nandal, S. L. Jain, Coord. Chem. Rev. 2022, 451, 214271.
- [6] Z. Wen, S. Xu, Y. Zhu, G. Liu, H. Gao, L. Sun, F. Li, Angew. Chem. Int. Ed. 2022, 61, e202201086; Angew. Chem. 2022, 134, e202201086.
- [7] S. Roy, M. Miller, J. Warnan, J. J. Leung, C. D. Sahm, E. Reisner, ACS Catal. 2021, 11, 1868–1876.
- [8] K. Sekizawa, S. Sato, T. Arai, T. Morikawa, ACS Catal. 2018, 8, 1405–1416.

5213773, 2023, 4, Downloaded from https://onlinelibrary.wiley.com/doi/10.1002/anie.20215213 by Yale University, Wiley Online Library on [08/06/2023]. See the Terms and Conditions (https://onlinelibrary.wiley.com/terms-and-conditions) on Wiley Online Library for rules of use; OA articles are governed by the applicable Creative Commons License



- [9] H. Kumagai, G. Sahara, K. Maeda, M. Higashi, R. Abe, O. Ishitani, *Chem. Sci.* 2017, 8, 4242–4249.
- [10] T.-T. Li, B. Shan, T. J. Meyer, ACS Energy Lett. 2019, 4, 629–636.
- [11] B. Kumar, J. M. Smieja, A. F. Sasayama, C. P. Kubiak, Chem. Commun. 2012, 48, 272–274.
- [12] K. Alenezi, S. K. Ibrahim, P. Li, C. J. Pickett, Chem. Eur. J. 2013, 19, 13522–13527.
- [13] E. Torralba-Peñalver, Y. Luo, J.-D. Compain, S. Chardon-Noblat, B. Fabre, ACS Catal. 2015, 5, 6138–6147.
- [14] L. Chen, Z. Wang, P. Kang, Chin. J. Catal. 2018, 39, 413-420.
- [15] J. J. Leung, J. Warnan, K. H. Ly, N. Heidary, D. H. Nam, M. F. Kuehnel, E. Reisner, *Nat. Catal.* 2019, 2, 354–365.
- [16] X. Zhang, Z. Wu, X. Zhang, L. Li, Y. Li, H. Xu, X. Li, X. Yu, Z. Zhang, Y. Liang, H. Wang, Nat. Commun. 2017, 8, 14675.
- [17] Y. Wu, Z. Jiang, X. Lu, Y. Liang, H. Wang, *Nature* **2019**, *575*, 630, 642
- [18] Y. Wu, Y. Liang, H. Wang, Acc. Chem. Res. 2021, 54, 3149– 3159.
- [19] S. Jiang, Z. Chen, X. Chen, D. Nguyen, M. Mattei, G. Goubert, R. P. Van Duyne, J. Phys. Chem. C 2019, 123, 9852–9859.
- [20] D. López-Díaz, M. López Holgado, J. L. García-Fierro, M. M. Velázquez, J. Phys. Chem. C 2017, 121, 20489–20497.
- [21] N. Majoul, S. Aouida, B. Bessaïs, Appl. Surf. Sci. 2015, 331, 388–391.

- [22] B. Shang, F. Zhao, C. Choi, X. Jia, M. Pauly, Y. Wu, Z. Tao, Y. Zhong, N. Harmon, P. A. Maggard, T. Lian, N. Hazari, H. Wang, ACS Energy Lett. 2022, 7, 2265–2272.
- [23] B. Shan, S. Vanka, T.-T. Li, L. Troian-Gautier, M. K. Brennaman, Z. Mi, T. J. Meyer, *Nat. Energy* 2019, 4, 290–299.
- [24] T. Arai, S. Sato, K. Sekizawa, T. M. Suzuki, T. Morikawa, Chem. Commun. 2019, 55, 237–240.
- [25] M. Zhu, R. Ye, K. Jin, N. Lazouski, K. Manthiram, ACS Energy Lett. 2018, 3, 1381–1386.
- [26] Y. Wu, G. Hu, C. L. Rooney, G. W. Brudvig, H. Wang, ChemSusChem 2020, 13, 6296–6299.
- [27] L. L. Shi, M. Li, B. You, R. H. Liao, Inorg. Chem. 2022, 61, 16549–16564.
- [28] X. Chen, D. Wei, M. S. G. Ahlquist, Organometallics 2021, 40, 3087–3093.
- [29] I. Roh, S. Yu, C. K. Lin, S. Louisia, S. Cestellos Blanco, P. Yang, J. Am. Chem. Soc. 2022, 144, 8002–8006.
- [30] D. Meroni, L. Lo Presti, G. Di Liberto, M. Ceotto, R. G. Acres, K. C. Prince, R. Bellani, G. Soliveri, S. Ardizzone, J. Phys. Chem. C 2017, 121, 430–440.
- [31] B. Wu, T. Wang, B. Liu, H. Li, Y. Wang, S. Wang, L. Zhang, S. Jiang, C. Pei, J. Gong, Nat. Commun. 2022, 13, 4460.

Manuscript received: October 17, 2022

Accepted manuscript online: November 29, 2022 Version of record online: December 20, 2022 5213773, 2023, 4, Downloaded from https://onlinelibrary.wiley.com/doi/10.1002/anie.20215213 by Yale University, Wiley Online Library on [08/06/2023]. See the Terms and Conditions (https://onlinelibrary.wiley.com/terms-and-conditions) on Wiley Online Library for rules of use; OA articles are governed by the applicable Creative Commons License